Field Survey and Numerical Modelling of the December 22, 2018 Anak Krakatau Tsunami

Jose C. Borrero,[1,2] Tubagus Solihuddin,[3] Hermann M. Fritz,[4] Patrick J. Lynett,[2] Gegar S. Prasetya,[5] Vassilios Skanavis,[2] Semeidi Husrin,[3] Kushendratno,[6] Widjo Kongko,[7] Dinar C. Istiyanto,[7] August Daulat,[3] Dini Purbani,[3] Hadiwijaya L. Salim,[3] Rahman Hidayat,[8] Velly Asvaliantina,[8] Maria Usman,[5] Ardito Kodijat,[9] Sangyoung Son,[2,10] and Costas E. Synolakis[2,11]

Abstract—On December 22, 2018, the eruption and flank collapse of the Anak Krakatau volcano generated a tsunami in the Sunda Strait causing catastrophic damage to uninhabited coastlines proximal to the source. Along the heavily populated shores of Banten and Lampung provinces in Java and Sumatra, tsunami waves caused severe damage, extensive inundation and more than 430 deaths. An international tsunami survey team (ITST) deployed 6 weeks after the event documented the tsunami effects including runup heights, flow depths and inundation distances, as well as sediment deposition patterns and impacts on infrastructure and the natural environment. The team also interviewed numerous eyewitnesses and educated residents about tsunami hazards. This ITST was the first to visit and document the extreme tsunami effects on the small islands in the Sunda Strait closest to Anak Krakatau (Rakata, Panjang, Sertung, Sebesi and Panaitan). Along the steep slopes of Rakata and Sertung islands, located less than 5 km from and facing directly towards the southwest flank of Anak Krakatau,

[1] eCoast Marine Consulting and Research, Raglan, New Zealand. E-mail: jose@ecoast.co.nz

[2] Department of Civil and Environmental Engineering, University of Southern California, Los Angeles, CA 90089, USA.

[3] Marine Research Centre, Ministry of Marine Affairs and Fisheries, Jakarta 14430, Indonesia.

[4] School of Civil and Environmental Engineering, Georgia Institute of Technology, Atlanta, GA 30332, USA.

[5] Indonesian Tsunami Scientific Community, Jakarta 12950, Indonesia.

[6] Center for Volcanology and Geological Hazard Mitigation, J1. Diponegoro no. 57, Bandung, Indonesia.

[7] Port Infrastructure & Coastal Dynamic Technology Center (BTIPDP), Agency for the Assessment and Application of Technology (BPPT), Jl.Grafika 2 Sekip, Yogyakarta 55284, Indonesia.

[8] Coordinating Ministry for Maritime Affairs, Jakarta 10340, Indonesia.

[9] IOC-UNESCO, Indian Ocean Tsunami Information Center (IOTIC), Jakarta 12110, Indonesia.

[10] School of Civil, Environmental and Architectural Engineering, Korea University, Seoul 02841, Republic of Korea.

[11] Department of Environmental Engineering, Technical University of Crete, 73100 Chania, Greece.

all of the dense coastal vegetation was stripped to bare earth up to elevations of more than 80 m, while on the northeast tip of Sertung Island, facing away from the source, a single tree remained standing after flow depths of > 11 m above ground struck there. The runup distributions on the islands encircling Anak Krakatau highlight the directivity of the tsunami source suggesting that the collapse occurred towards the southwest. This manifested as tsunami runup of < 10 m on Sebesi Island, located 15 km northeast of the source, contrasting with tsunami flow heights > 10 m that stripped away coastal forests to bare rock for up to 400 m inland in the Ujung Kulon National Park, located 50 km to the southsouthwest. Inundation and damage were mostly limited to within 400 m of the shoreline, likely the result of the relatively short wavelengths caused by the landslide generated tsunami. A significant variation in tsunami impact was observed along the shorelines of the Sunda Strait, with runup heights rapidly decreasing with distance from the inferred tsunami source. To model the event we applied a hot-start initial condition that roughly reproduced the measured tsunami runup heights along Rakata and Sertung. The waveforms were then propagated through the Sunda Straight using a Boussinesq-type wave model. The results showed a good fit to the observed heights along the Java and Sumatra coastlines, the northern coast of Panaitan Island and Ujung Kulon Nation Park. The model also produced an acceptable fit to the observed amplitudes at tide gauges. Despite the regional volcanic and tsunamigenic history of the region, and 6-months of eruptive activity prior to the event, the tsunami largely caught the local population off guard. This further highlights the need for community-based education and awareness programs as essential to save lives in locales at risk from locally generated tsunamis.

1. Introduction

On December 22, 2018, an eruption and partial collapse of the Anak Krakatau volcano generated a tsunami in the Sunda Strait (Fig. 1). According to the Indonesian National Disaster Management Authority
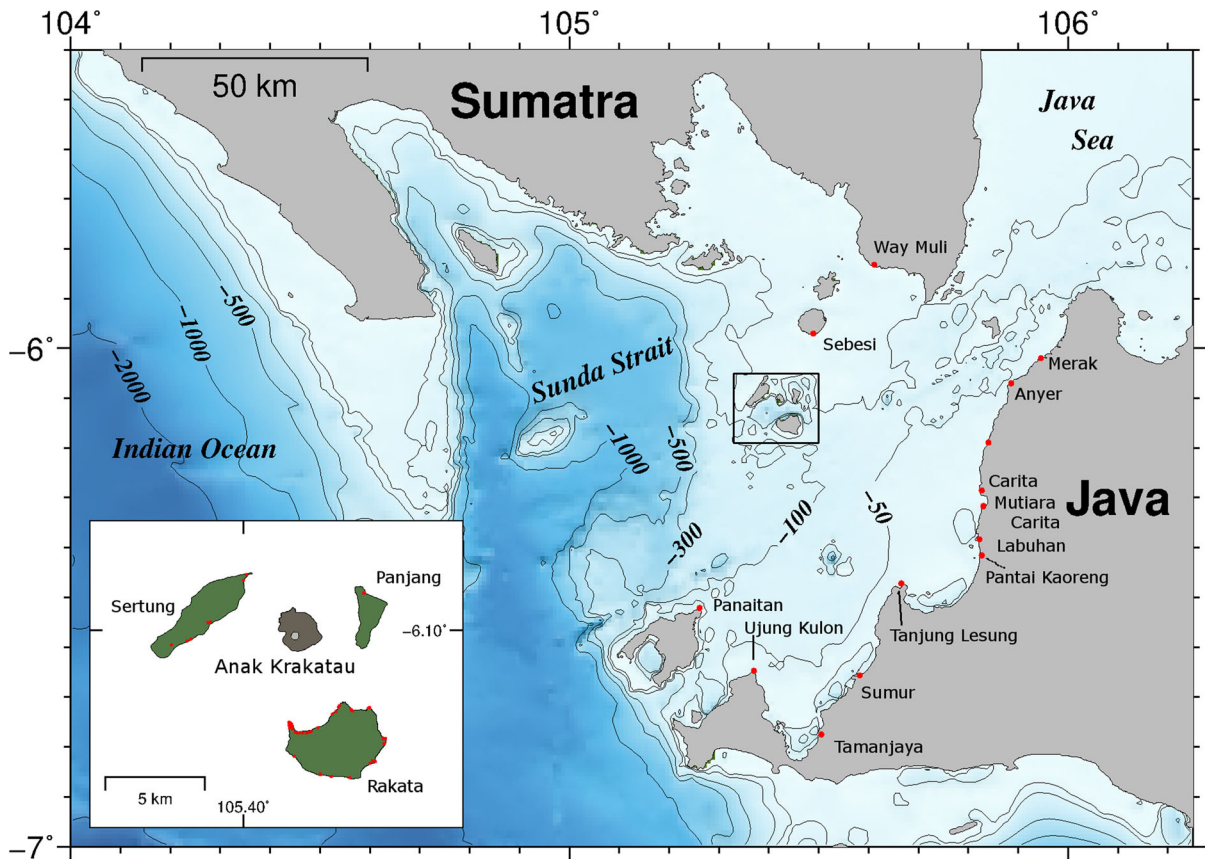
Figure 1
Location map. Inset shows the area around Anak Krakatau in more detail. Shorelines are digitized from post-event satellite imagery. Red dots are locations where measurements were made

(BNPB), the 22 December 2018 tsunami caused over 430 fatalities, injured 14,000 people, and displaced 33,000 more along the Sunda Strait. The tsunami caused catastrophic damage in coastal regions of the Sunda Strait in Lampung (Sumatra) and Banten (Java).

Immediately following the event, which was widely reported in the international media, Indonesian and international survey teams recorded the effects of the tsunami, however these efforts focused mostly on the western coast of Java and somewhat on the southern coast of Sumatra (Muhari et al. 2019; Putra et al. 2020).

It was not until an international tsunami survey team (ITST) was deployed 6 weeks after the event that the effects in the immediate source area were quantitatively recorded. This ITST effort worked with Indonesian teams to systematically document flow depths, runup heights, inundation distances, sediment deposition, impact on the natural environment and infrastructure.

1.1. History

The Krakatau stratovolcano was formed by the subduction of the Indian-Australia Plate under the Eurasian Plate. At its peak, the island of Rakata, which the volcano of Krakatau had formed, had reached a height of more than 800 m above sea level. According to ancient Javanese scriptures, the first recorded eruption of Krakatau occurred in the year 416 AD, though some have reported in 535 AD (Pararas-Carayannis 2003).

The eruptions of Krakatau on 26 and 27 August 1883 were the culmination of volcanic activity ongoing since May of that year resulting in one of

the deadliest volcanic eruptions of modern history. It is estimated that > 36,000 people died, many because of the tsunami following the largest eruption which occurred on the morning of August 27 (Verbeek 1885; Self and Rampino 1981). This eruption resulted in the complete collapse of the volcano and the formation of a submarine caldera where the island previously existed.

After nearly 43 years of relative quiescence, on 29 December 1927 a new explosion on the sea surface was recorded at the center of the caldera formed after the 1883 eruption. Explosions continued until 15 January 1929 and formed the small island of Anak Krakatau. Since its first appearance above the sea surface in 1927 through 2005, the elevation of Anak Krakatau grew to 315 m (Sutawijaya 2006), and up to 338 m in 2018 before its most recent eruption on 22 December 2018. Following this last eruption the elevation of Anak Krakatau has dropped to 110 m above sea level (Kushendratno 2019).

1.2. The Eruption and Flank Collapse of December 22, 2018

The details of the eruptive activity that culminated in the flank collapse, landslide and subsequent tsunami are discussed in detail in Walter et al. (2019). They analyzed several different data sets and described Anak Krakatau's elevated state of activity prior to the tsunamigenic flank collapse. This included thermal anomalies, an increase in the island's surface area, and a gradual seaward motion of its southwestern flank on a dipping décollement. The most recent phase of activity at Anak Krakatau began in June 2018 and was the most intense recorded since systematic observations began in 2000 (Walter et al. 2019). According to their analysis, the tsunamigenic flank collapse itself occurred at 13:55 UTC and was preceded by high levels of volcanic activity, followed by a brief quiet period. A small seismic event at ∼ 13:53 UTC was followed by a much larger signal 115 s later, interpreted by Walter et al. (2019) as the landslide itself. Their analysis suggests that the landslide lasted approximately 1 min and had a moment magnitude of 5.3 with a

significant non-double-couple component oriented toward the southwest with a dip angle of 12°.

2. Field Survey

An initial survey of the tsunami effects was carried out by Muhari et al. (2019) and Putra et al. 2020. These surveys focused on the mainland shores of Sumatra and Java reporting tsunami flow depths of 2–4 m on the southern coast of Sumatra, and 0.5 to nearly 7 m along the western side of Java from Anyer to Sumur, with significant spread in the measured values at each site. In terms of runup, they measured 3–7 m in the vicinity of Labuhan and Carita and 7–13.5 m runup heights at the northern tip of the Tanjung Lesung Peninsula.

Generally their data suggests that the hardest hit areas were in the vicinity of Carita Beach, Tanjung Lesung and Sumur. No measurements in the immediate source area or on other islands nearby such as Sebesi were reported. There were no reported measurements from the north facing coasts of Panaitan Island and the Ujung Kulon National Park. These areas faced directly towards the assumed tsunami source. Preliminary numerical modelling suggested they would have been affected by tsunami heights larger than those which affected the western coast of Java.

For this reason, an ITST comprised of Indonesian and International scientists visited the area from 4 to 9 February, 2019. After obtaining the necessary permits, the team worked to gather additional tsunami data from the Java mainland and travelled by boat to survey the effects on the small islands near the source region, Panaitan Island and Ujung Kulon 50 km to the south, Sebesi Island 20 km to the north and one site along the southern coast of Sumatra.

At each site, measurements and interviews were collected using established protocols (i.e. UNESCO 2014). Runup heights, inundation distances and flow depths are defined in Fig. 2. Measurements were taken using a laser rangefinder and a Trimble GPS with differential correction. Given the nature of the boat survey and the distance to the permanent base station on Java of 100–200 km, the elevations were referenced to the sea level and de-tided for the time of
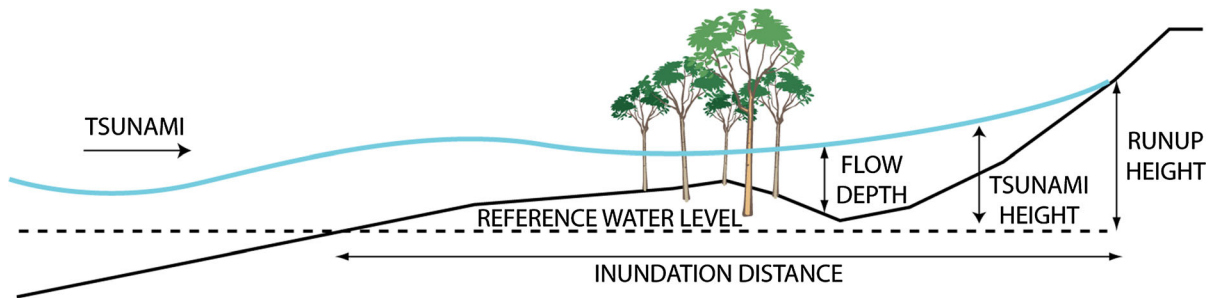
Figure 2
Definition sketch for flow parameters measured during the field survey

tsunami arrival. The complete set of measured runup, flow depth and inundation distances are provided in in the supplementary material.

2.1. Western Java

Several locations were surveyed along the western coast of Java Island as indicated in Fig. 1.

2.1.1 Anyer

At Anyer, several interviews conducted with local workers suggested that the tsunami effects consisted of a rise in the water level of up to 2 m, with inundation less than 10 m from the coastline. Damage in this area was not significant, as lightly constructed vendor stalls made of bamboo remained intact and standing (Fig. 3).

2.1.2 Labuhan

At Labuhan, one witness reported four waves with the largest 'as high as an adult male' (~ 1.8 m). He reported that the first wave inundated to a level roughly equivalent to a high tide, while the second wave a few minutes later hit him and inundated his fruit stall. The third wave also caused flooding, while the fourth wave was smaller. He also reported that after the fourth wave the water receded quickly.

At the Labuhan fish market, the tsunami was approximately 1 m high and occurred when the market was still crowded with visitors, inundating up to 200 m inland. However, damage only occurred within approximately 10 m of the shoreline.

Tsunami monitoring equipment installed at Labuhan in 2012 by BMKG (Indonesia's Meteorological, Climatological and Geophysical Agency) and a tide gauge for tsunami monitoring were spotted, however both pieces of equipment appeared to be abandoned

Figure 3
Pasauran Beach, Anyer, 24 December 2018. Vendor stalls are still intact suggesting relatively benign tsunami impacts

and non-functional. Locals reported that a tsunami evacuation siren installed on the pier in Labuhan had sounded periodically for preparedness drills, however during this event it was not activated.

A multi-story vertical evacuation structure had been built in Labuhan, as shown in Fig. 4, however it appears abandoned and not well maintained and most of the residents seemed confused when asked about the function of this building.

2.1.3 Mutiara Beach, Carita

There was significant tsunami damage at Mutiara Beach where a beachside hotel was heavily impacted. There were reports of 70 casualties, most of them visitors. The damage here was severe with many buildings exhibiting classic tsunami damage where lower story walls were blown out in the direction of the flow (Fig. 5).

2.1.4 Sumur

At Sumur the survey focused on the lagoon area which was most affected by the tsunami. Here the damage was severe with all buildings destroyed within 100 m of the shoreline. This observation also was reported by the Heidarzadeh et al. (2020b) field survey. Based on the interviews and observations, we concluded that the tsunami approached from the west-southwest and consisted of three waves. The first wave was relatively small but reached higher than a typical high tide. The second wave was reported larger than the first, while third was about the same as the second. However, when the third wave came, people were already running to escape to higher ground. Tsunami runup was 5–6 m with maximum inundation distances of approximately 200 m. Damage was severe with most buildings destroyed including relatively sturdy brick and cement structures (Fig. 6).

2.1.5 Tanjung Lesung Resort

The beach club at Bodur Beach suffered considerable damage with most buildings damaged or destroyed. A wharf used for boat embarkation was also destroyed (Fig. 6). Witness accounts indicated three waves, a smaller first wave was followed by larger and more destructive second and third waves. Tsunami runup was 3–4 m with inundation distances of 150–200 m. This was indicated by damaged buildings and trees with most of the damage concentrated in the first 50 m from the shoreline.

2.2. Survey of Islands in the Immediate Source Region

On February 5 and 6, 2019, the survey team visited the cluster of islands in the immediate vicinity of Anak Krakatau. To the south lies Rakata, whose ~ 800 m peak is the only remnant of the Krakatau volcano that erupted in 1883. To the west, lies Pulau Sertung and to the east Pulau Panjang

Figure 4
Tsunami warning infrastructure (left) and a vertical evacuation structure (right) in Labuhan

Figure 5
Damage at Mutiara Carita Beach

(Fig. 1). On subsequent days, the team also visited Sebesi 20 km to the north and Panaitan and Ujung Kulon 50 km to the south.

2.3. Rakata, Sertung and Panjang

Starting on Rakata, the team first landed on the eastern coast in a cove somewhat protected and facing away from the tsunami source area. Here the team measured runup and tsunami heights of 6–10 m. Moving to the larger, northwest facing embayment revealed a clear tsunami trim line extending across the entire length of the embayment (Fig. 7). Measured tsunami heights increased from east to west starting at over 10 m and increasing to 85 m before dropping off again to $\sim$ 50 m at the northwestern tip of Rakata. Circling the island by boat, the team measured runup heights generally between 4 and 12 m on the shorelines facing away from Anak Krakatau, with the notable exception of two points of $\sim$ 20 m runup on the southern coast, facing directly away from the tsunami source region. This could possibly be the effect of constructive interference from the tsunami wave fronts wrapping around Rakata and meeting each other on the back side of the island, as observed on Babi Island during the surveys

of the Flores, Indonesia tsunami of 1992 (Yeh et al. 1993) and reproduced in the laboratory experiments of Briggs et al. (1995), in the numerical results of Liu et al. (1995) and the analytical results of Kanoglu and Synolakis (1998).

The team next visited Pulau Panjang (Fig. 8), the island situated to the east of Anak Krakatau. Here a boat landing was only possible on the northern coast where tsunami inundation and runup were measured at 7 to 9 m. The island itself was covered with fresh ash deposits, the trees had lost most of their leaves with only snags remaining and the entire landscape appeared to have been 'cooked'. We attribute this to the hot ash from the eruption which was blown over the island by the prevailing southwesterly winds for a period of days following the eruptions. Along the western shore of Panjang there was evidence of tsunami runup and small-scale landslides which could have been caused by tsunami uprush.

One landing was made on the northwestern shore of Anak Krakatau itself. Here there were no measurable traces from which to deduce a tsunami runup height. However the freshly deposited ash layer had been obviously already eroded by wave activity owing to the vertical scarp present at the shoreline.

Figure 6
(top row) Damage at Sumur. (bottom row) Damage at Tanjung Lesung Peninsula showing a damaged beach club building and the destroyed wharf

Along the northwestern tip of Pulau Sertung (Fig. 9), the team measured tsunami runup of 26 m which penetrated about 50 m up a small ravine. The extreme tip of the island was covered with a deep layer of pumice. A stand of trees which had existed there had been sheared off at their base, presumably by the tsunami. A lone standing tree exhibited evidence of tsunami impact and had large chunks of bark stripped off up to heights of > 10 m above ground level and broken branches at 14 m elevation, suggesting this value as a minimum flow depth.

Along the south facing coast of Sertung there was clear evidence of extreme tsunami effects with all the vegetation stripped off the steep coastal bluffs up to an elevation of 83 m in one location. This trim line was relatively consistent across the entire southern

shore of the island. The measured tsunami runup heights from Rakata and Sertung are plotted in Fig. 10.

2.4. Pulau Sebesi and the Southern Coast of Sumatra

The survey team also travelled to Pulau Sebesi and Waymuli on the southern coast of Sumatra. Pulau Sebesi, with a population of approximately 3000 people is located approximately 20 km north of Anak Krakatau. The majority of Sebesi residents live in Regan Laga Village, located on the eastern side of the island or near the port situated on the northeastern side of Sebesi.
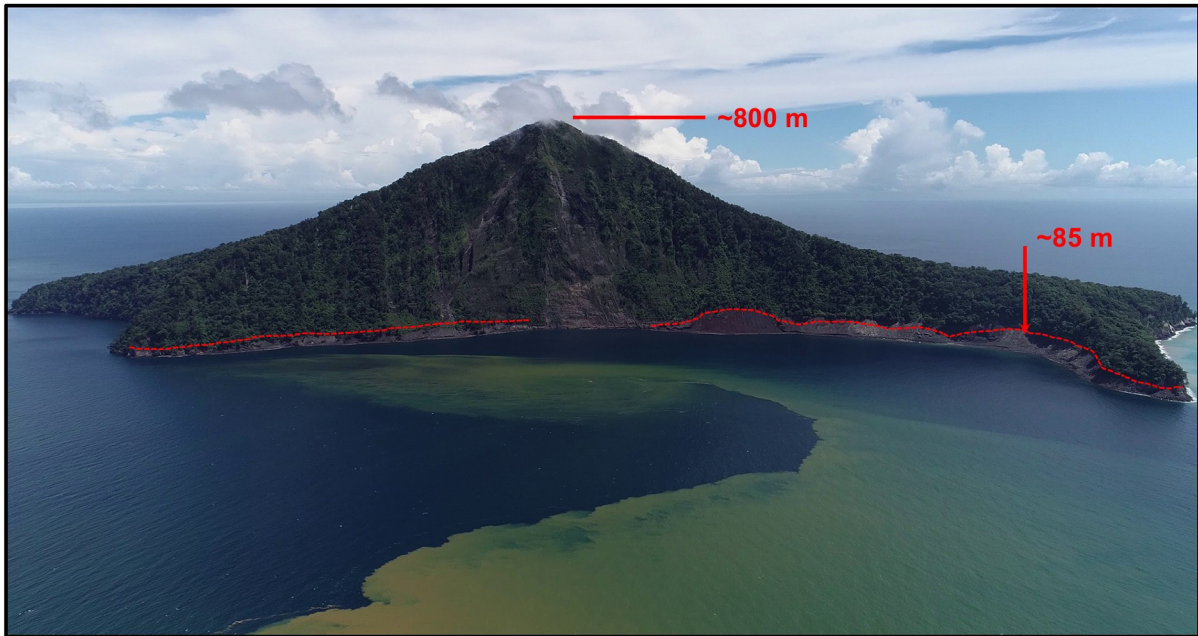
Figure 7
Rakata Island. The tsunami trim line is shown in dashed red and the location of the high runup point of ∼ 85 m is indicated. See Fig. 1 inset for location relative to Anak Krakatau

Based on interviews with residents having a direct view of the Anak Krakatau volcanic complex, the tsunami wave occurred shortly after the eruption at around 09:15 PM and was accompanied by a thunderous sound from the direction of the volcano. The tsunami waves hit Sebesi Island three times in the form of short waves with a period of less than 5 min, with the first wave being the largest. The most affected area was along the southern coast of Sebesi where runup and inundation were measured at up to 9 m and 130 m, respectively. Several houses along the southeastern coast were destroyed by the tsunami waves. There was also evidence of large coral boulders (one measured at 2.2 m long, 1.2 m wide and 1.2 m high, Fig. 11) displaced from the offshore reef and deposited 40 m inland, a total of ∼ 100 m from its original location. Coral boulder transport at sites in western Java was also reported in the survey of Putra et al. (2020).

Waymuli is a rural area located on the southern coast of Sumatra Island, approximately 40 km from Anak Krakatau. Eyewitness accounts suggest that the tsunami was comprised of four waves, which arrived at approximately 9:30 PM. As with Sebesi, eyewitnesses reported that the first wave was the largest. Tsunami runup was measured at 4.25 m with inundation of up to 100 m. The damage at Waymuli was severe with a large number of buildings damaged or destroyed between the seafront and the coastal road (see Fig. 11). By the time this survey was conducted, much of the debris had been cleared away.

2.5. Pulau Panaitan and Ujung Kulon National Park

Preliminary modelling of the tsunami propagation patterns emanating from Anak Krakatau provided to the tsunami community shortly after the event (S. Grilli pers. comm) suggested that the tsunami effects would be strongly focused towards the northern tips of Panaitan Island and Ujung Kulon National Park located some 50 km south of Anak Krakatau at the extreme western end of Java Island. Indeed, upon landing at these sites, it was clear the tsunami effects were extreme, particularly at Ujung Kulon where every bit of what was once dense tropical forest was

Figure 8
(top) Aerial view of Panjang Island to the north east of Anak Krakatau. Note the dead forest. (bottom) View from above the northern end of Panjang towards the southwest over Anak Krakatau. Sertung to the right and Rakata to the left with the tsunami runup scar/trimline clearly visible. See Fig. 1 inset for relative locations

stripped away leaving behind only coral rubble (Fig. 12).

On Panaitan, the ITST measured tsunami flow depths of 5–7 m with inundation of up to 350 m

whereas at the northern tip of Ujung Kulon, flow depths at the shoreline were at least 9.1 m (Fig. 13).

Due to time constraints, we were unable to survey to the full inundation extent, however, inspection of
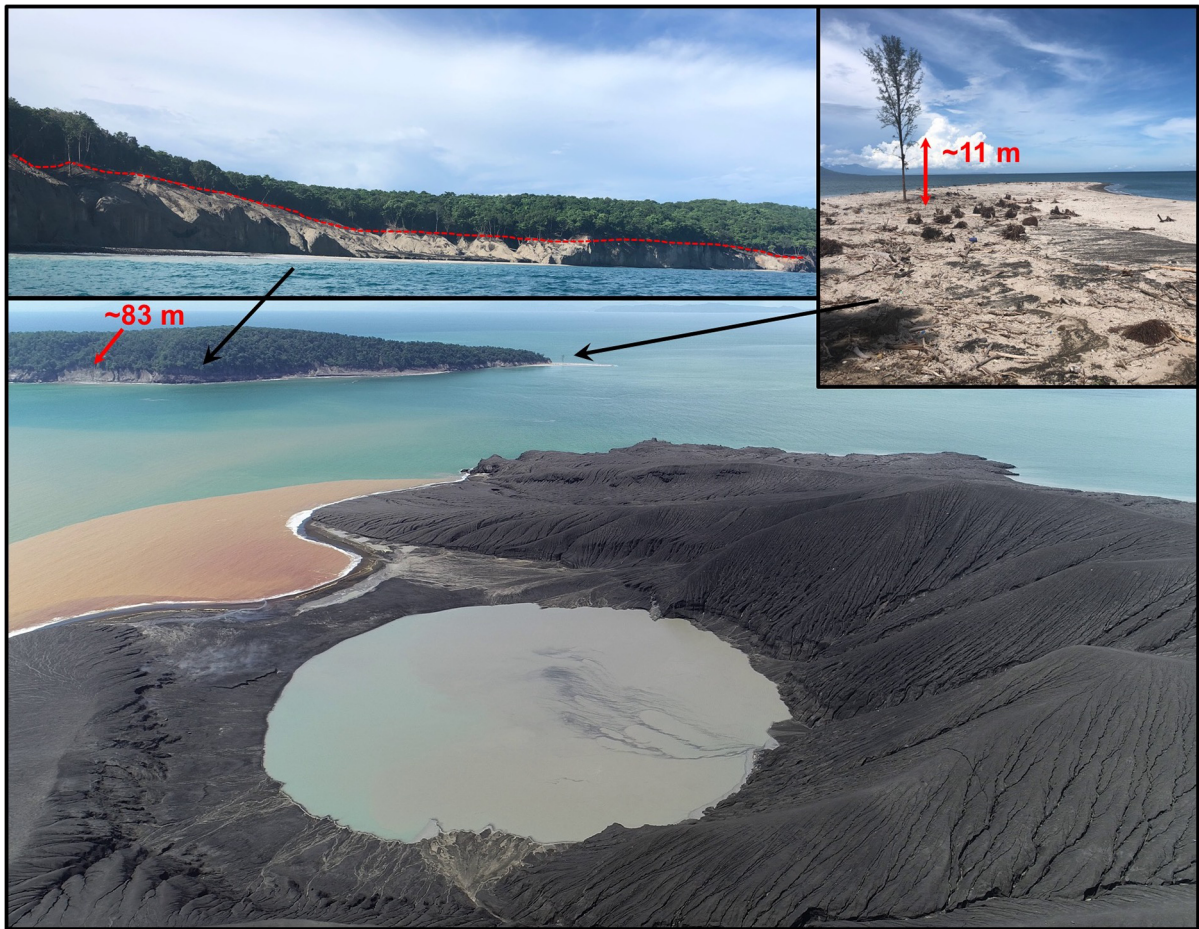
Figure 9
(top right) The lone tree on the northeast tip of Sertung where the tsunami completely over washed the sandspit. (top left) The tsunami trim line is indicated in red. (bottom) The location of the maximum runup height of 83 m as seen from the direction of Anak Krakatau

publicly available satellite imagery (i.e. Google Earth) suggests a minimum inundation distance of the order of 800 m along the axis of the north facing peninsula at Ujung Kulon with 200–400 m inundation along the northwestern facing shore. The inundation effects at the northern tip of Ujung Kulon were reminiscent of the extreme overland flows at Aonae Cape, Okushiri Island following the Hokkaido-Nansei-Oki earthquake on July 12, 1993 (Titov and Synolakis 1997).

2.6. Evaluating Hazard Awareness Amongst the Local Population.

Nationwide media coverage on tsunami threat in the area a few months earlier and the heightened volcanic activity preceding this event seemed to have little impact on the overall public awareness.[1] The ITST conducted several interviews throughout the survey area including at markets, in households and at primary and secondary schools. People interviewed included fishermen, merchants, families as well as primary and secondary school teachers.

---

[1] https://news.detik.com/berita/d-3957469/analisis-potensi-tsunami-57-m-bikin-resah-bppt-dipanggil-polda.
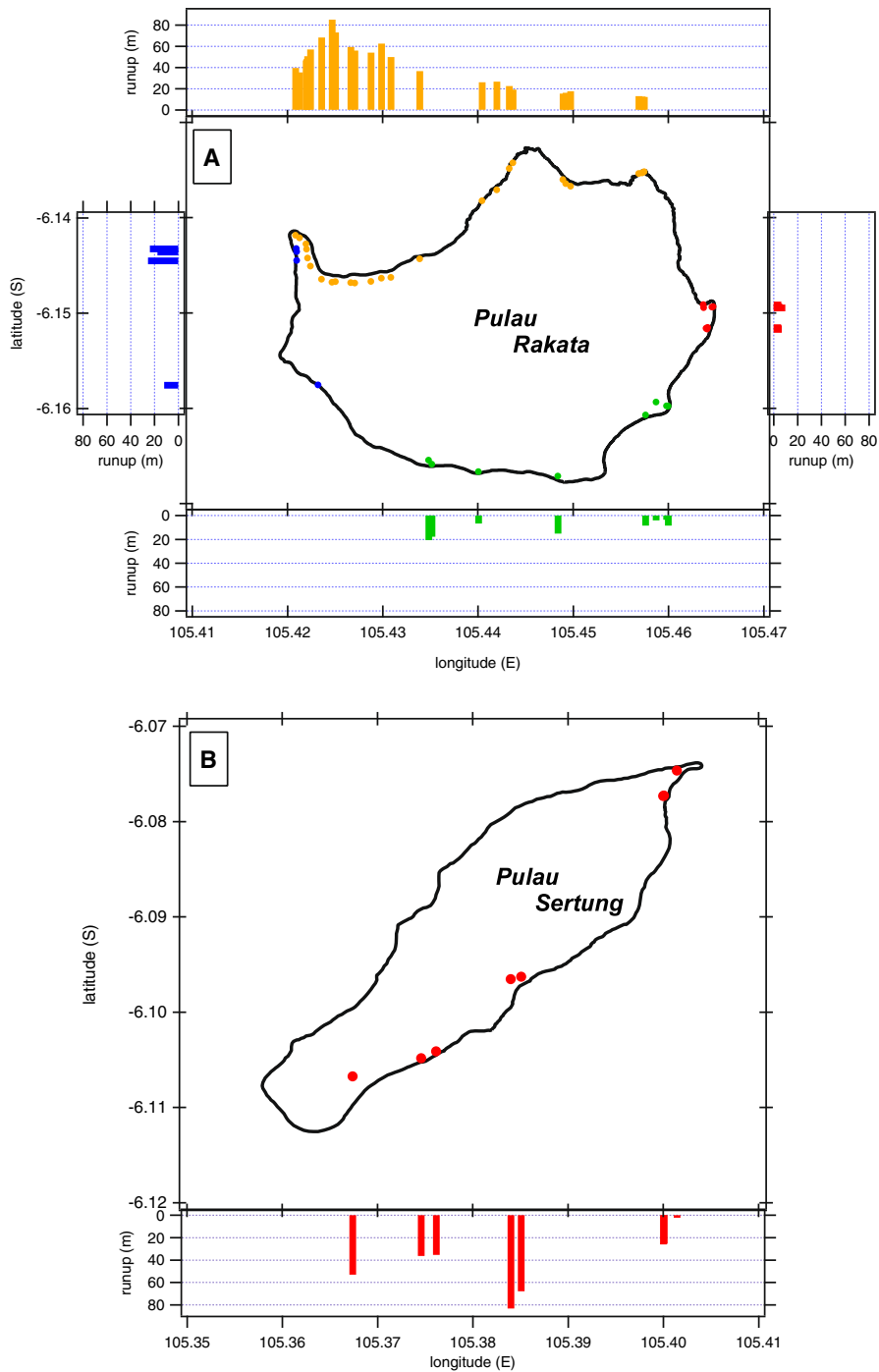
Figure 10
Measured tsunami heights on Rakata (**a**) and Sertung (**b**)

Overall, the assessment suggested that the general population was clearly not prepared for a tsunami disaster, particularly one without an obvious

earthquake, much as they were aware of the tsunami associated with the 1883 eruption. Amongst teachers and students in Sumur, the preparedness level was
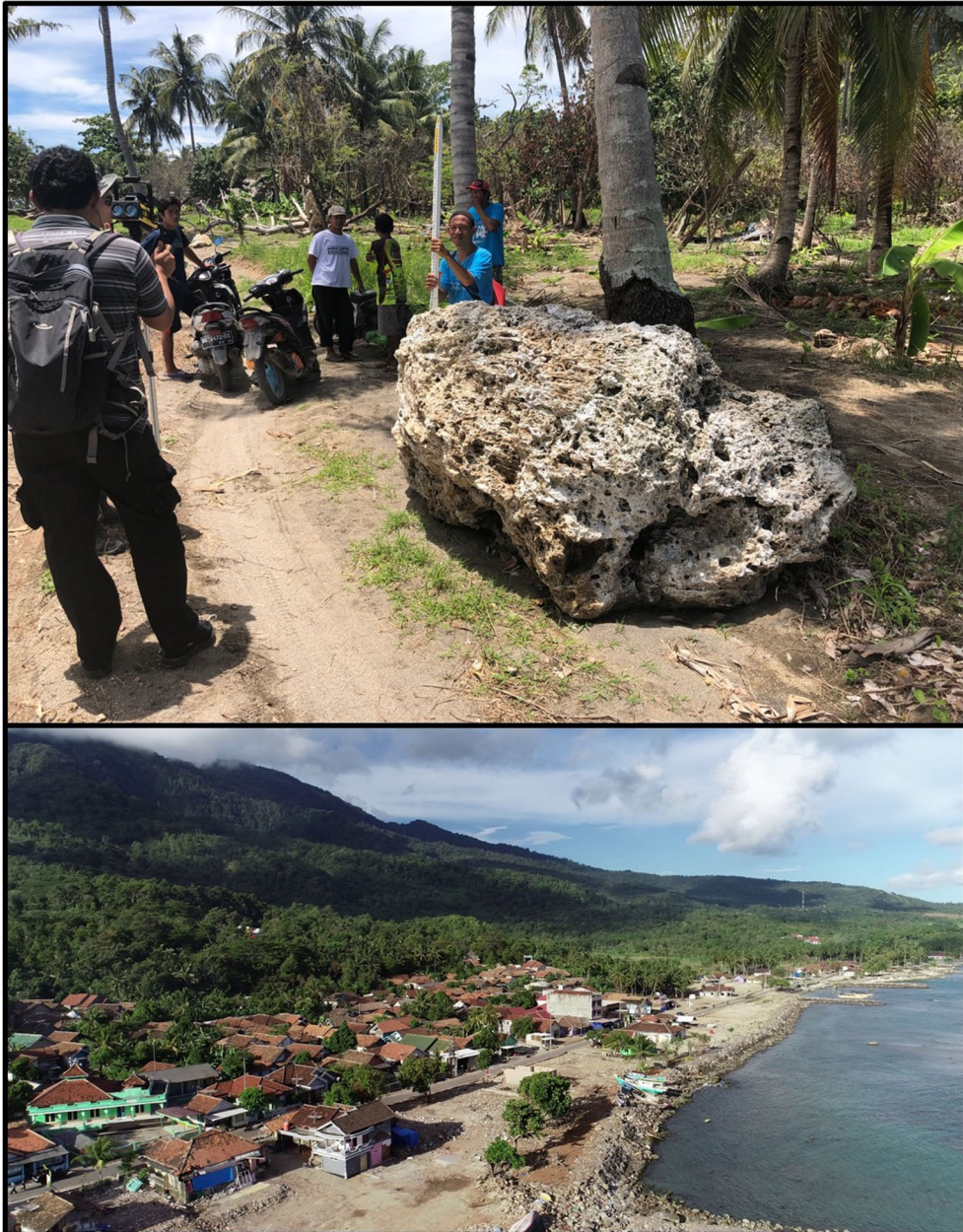
Figure 11
(top)On Sebesi, a large coral boulder displaced from ∼60 m offshore was transported some 40 m inland. (bottom) The heavily damaged Waymuli water front. Much of the debris had been cleared away by the time of the survey, hence the open areas at the shoreline

somewhat higher, and this may be due to ongoing educational initiatives related to natural disaster preparedness. Despite this bright spot, the people of West Java appear generally unprepared for tsunami disasters.

3. Numerical Modelling

A tsunami generated by a hypothetical flank collapse at Anak Krakatau was modelled by Giachetti et al. (2012) who proposed a scenario similar to that which transpired on 22 December 2018. Their

Figure 12
The northern tip of Ujung Kulon. Inset images show the height of flow depth traces left on a lone surviving tree and the location of the twisted remains of a steel navigation light that was previously installed at the shoreline

modelling featured a dynamic source model for a 0.28 m³ flank collapse coupled with a 2-D depth averaged hydrodynamic flow solver and water wave propagation model. Their results predicted tsunami heights of $\sim$ 45 m in the nearfield and runup heights of 1.5 m in Merak and 3.4 m in Labuhan. While this work was remarkable in its prescience, it underpredicted what actually transpired in 2018. Nonetheless, it should have been used as a benchmark for enhancing emergency preparedness.

Grilli et al (2019) used a suite of landslide sources with volumes between 0.22 and 0.3 km³ in a 3D slide and nearfield hydrodynamic model. Their modelling produced somewhat larger initial tsunami heights than Giachetti et al. (2019) and a good fit to coastal tide gauges in the Sunda Strait.

More recently, Heidarzadeh et al. (2020a) derived source parameters for the tsunami using qualitative physical modeling and wavelet analyses of the tsunami signal on coastal tide gauges. Their work suggested that the tsunami source was roughly circular monopole with an initial tsunami height of 100–150 m located just offshore to the southwest of

Anak Krakatau. Paris et al. (2020) also modelled the 2018 Anak Krakatau tsunami using a 2-D depth integrated simulation with the slide modelled as a granular flow for the initial wave generation and a Boussinesq model for the wave propagation.

In our modeling, we used the landslide initial conditions model of Lo and Liu (2017), based on analytical solutions of the linear, shallow water wave equations. Their inputs include the slide geometry, slide slope properties, and an estimate of the initial slide acceleration, here taken as solid body motion. The initial tsunami waveform derived from the Lo and Liu formulation is placed as a hot-start initial condition in the pCOULWAVE hydrodynamic model (Lynett 2006), which provides the evolution of the landslide-generated tsunami throughout the Sunda Strait. The Lo and Liu formulation estimates the tsunami after leaving the immediate source area above the landslide, and provides both the free surface elevation and horizontal velocity field for the pCOULWAVE initial condition.

A trial and error process was used to select and modify the source parameters until an acceptable fit
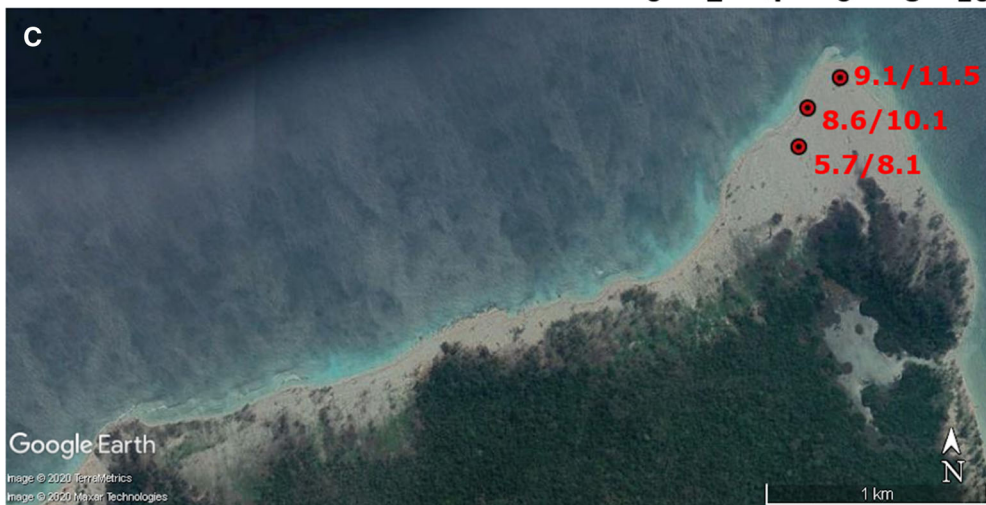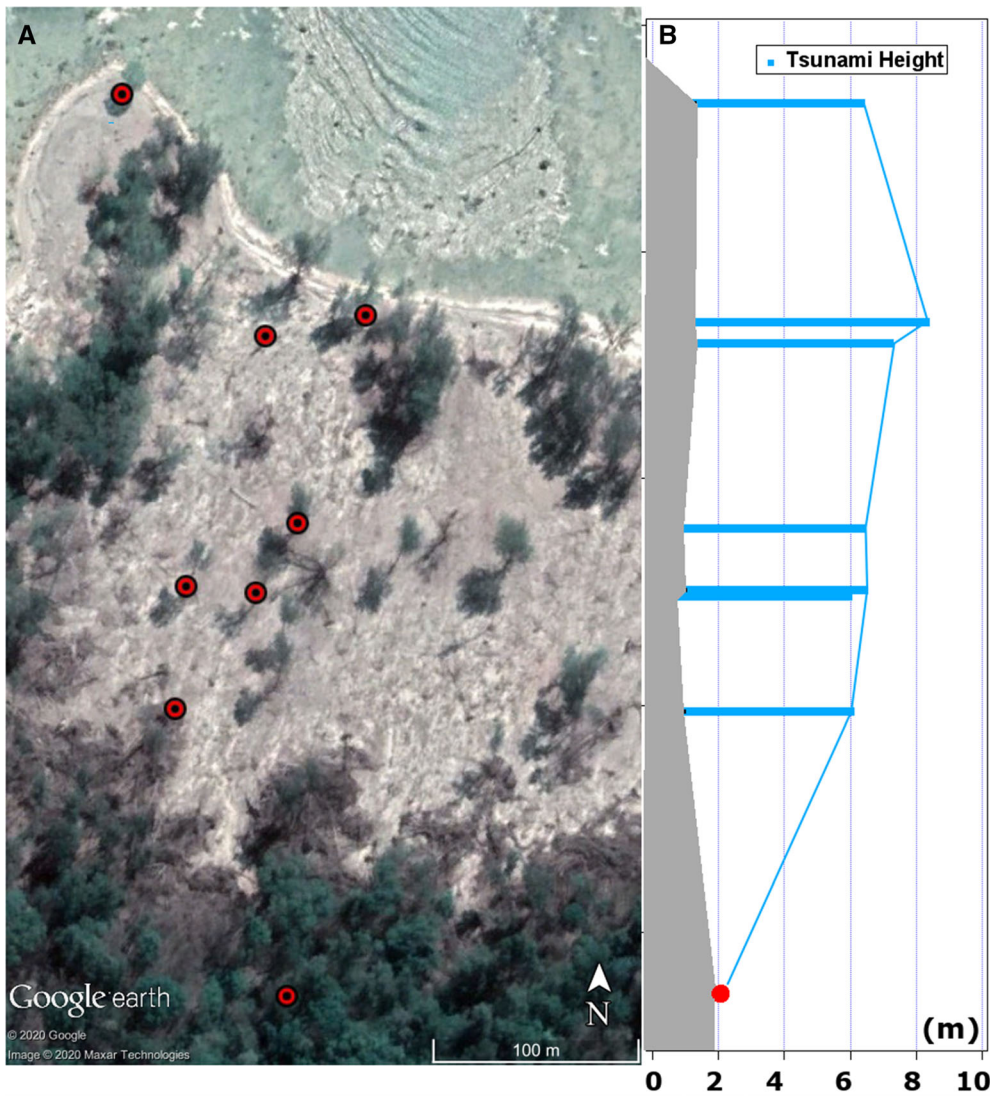
a Locations of measured tsunami runup and flow depths at the northern tip of Panaitan Island. **b** Tsunami height at each point in A indicated with the blue bars over ground level (gray shaded area). Red dot indicates the location of the end of the inundation extent along the transect. **c** Data point locations from the northern tip of Ujung Kulon. Numbers indicate tsunami flow depth over ground and total tsunami height above sea level respectively. The inundation zones at both sites are easily identified by the light colored areas which are bare coral rock. Prior to the tsunami both sites were covered with dense tropical forest to the shoreline

to the observed near field tsunami run up heights was found. Ultimately, the source parameters listed in Table 1 were used to generate the initial tsunami source depicted in (Fig. 14). This solution is used to provide order of magnitude estimates for the generated crest elevation and horizontal length scales and is not meant to capture the complex source dynamics of the Anak Krakatau failure.

A single pCOULWAVE model grid, with resolution of 2 arcsec (approximately 60 m), covers the Sunda Strait; nested grids were not used in these simulations. Bottom friction is approximated with Manning's formulation and a spatially constant "n" value of 0.025 $m^{1/3}$. Model results showing maximum computed tsunami amplitude close to the source are shown in Fig. 14. The modelled runup heights are compared to the measured field data on Rakata and Sertung in Fig. 14c, d. The model produces results generally consistent with the measured runup, however the model noticeably misses the extreme runup peak measured on Rakata. This discrepancy is likely due to errors in the available bathymetry and topography in this location or errors in the initial tsunami

Table 1

Landslide geometry and material source parameters used in the Lo and Liu (2017) formulations

Parameter	Value
Slope (β, °)	20
Thickness (A_b, m)	200
Length (L_b, m)	1000
Width (W, m)	1000
Depth (d_0, m)	150
Spec. Grav. (γ)	2.65
Drag Coef. (C_d)	1.5

condition. With the field data provided here at these locations, future researchers will be able to investigate these competing errors, and determine what data is needed to recreate the extreme runup on the islands.

Figure 15 provides the simulated tsunami propagation results through the Sunda Strait. The model results are generally in agreement with the field observations showing strong focusing of the tsunami height towards the northern tip of Ujung Kulon Park and to the Way Muli area on Sumatra, as can be seen in Fig. 15a. Model results are then compared to the measured tide gauge data in Fig. 15b, c. The measured data as presented here is the average of two tidal sensors at each of the two locations, as described in Grilli et al. (2019). The fit between the measured and modelled data is quite good at the Jambu Marina tide station. However, the results from the Ciwandan tide gauge are not as accurate. Although the model predicts the correct range of amplitudes, the timing of the peaks and troughs is not as good as at Jambu.

The modelling results presented here show an extremely steep and nonlinear wave in the source region with rapidly radial spreading of energy. There is clear directionality of energy to the southwest, indicating that the largest waves in the nearfield did not directly approach any of the coastlines of Rakata, Sertung, and Panjang. As the tsunami propagated away from the source region, frequency dispersion, radial energy spreading, and refraction control the local amplification of the tsunami amplitude. In the far field, the modelling captures the observed areas of focusing to the south (e.g. Ujung Kulon), east (e.g. Bodur Beach), and to the north (e.g. Way Muli). As shown, and as is typical for earthquake tsunami hazard assessments, the precise detail of the source and initial waves, which is disregarded here, is not of leading order importance for far-field predictions.

3.1. Comparison to the Tsunamis of 1883

The Krakatau eruptions of 26–27 August 1883 produced multiple tsunamis over the course of the event (Self and Rampino 1981). The largest of these occurred in the late morning of August 27 causing extensive destruction along the coasts of Java and Sumatra. Maximum tsunami runup heights from this
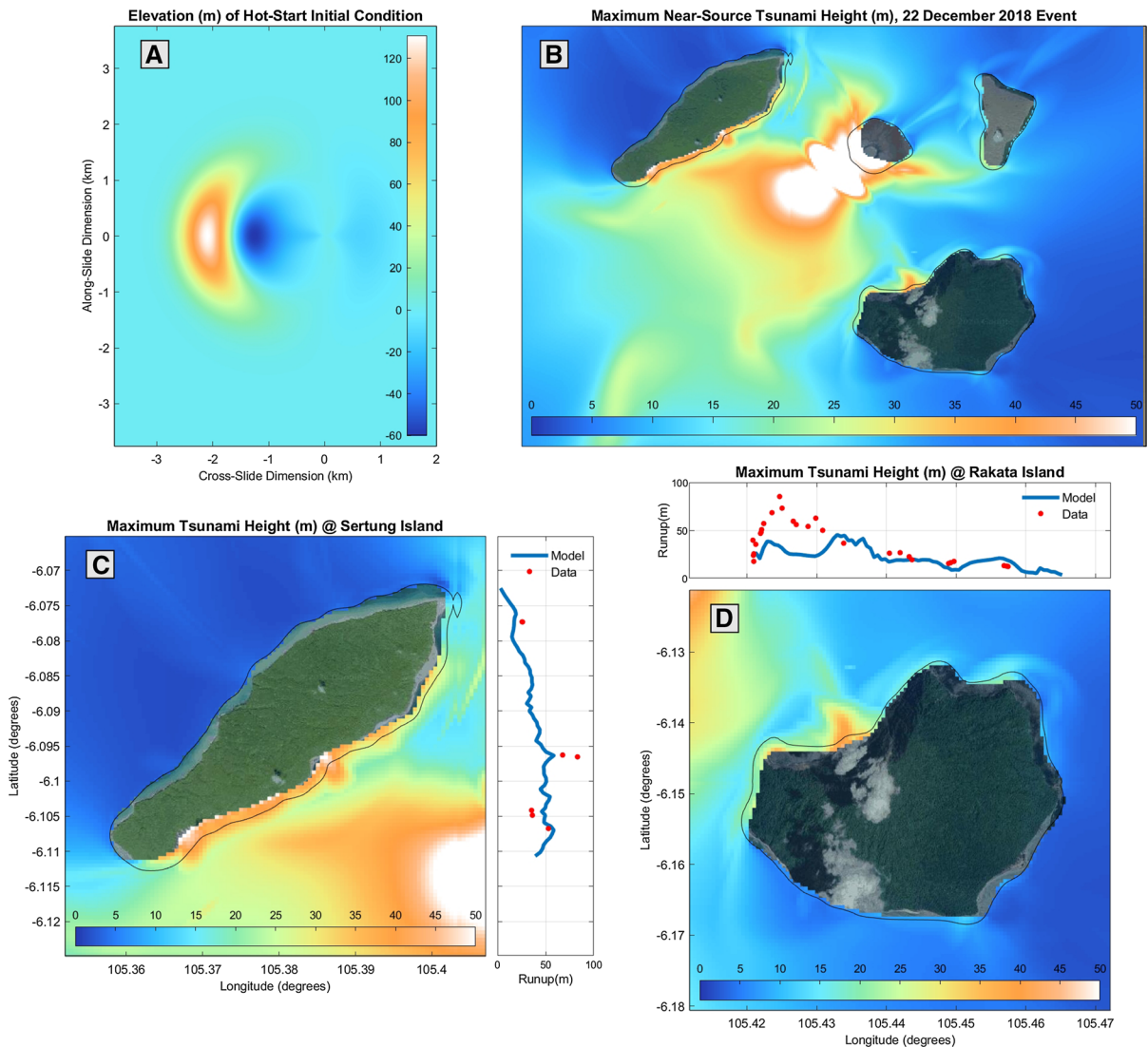
Figure 14
Initial water surface used as a hot-start initial condition in the numerical model (**a**), and near-field propagation of the tsunami (**b**–**d**). Subplot **b** provides the maximum tsunami amplitude near the source, while **c** and **d** are focused on Rakata and Sertung, respectively, and show the numerical-field data runup comparisons

event are reported in the literature and databases to be of the order of 30–40 m (i.e. Pararas-Carayannis 2003; NGDC/NCEI/WDS 2020). In contrast, the 2018 event will be referenced as having produced maximum tsunami runup of 85 m, thereby presenting the possibility of future researchers making false comparisons between the two events. It is therefore important that future studies discussing the tsunamis caused by Krakatau differentiate between runup data

collected from the shores of Sumatra and Java and runup on the islands near the source.

The only quantitative estimates of the near source tsunami amplitude or height for the 1883 come from efforts to numerically model the tsunami effects with values ranging from initial heights of 'more than 100 m' (Mader and Gittings 2006) to + 270 m or + 290 m (Nomanbhoy and Satake 1995; Maeno and Imamura 2011) for a phreaotomagmatic
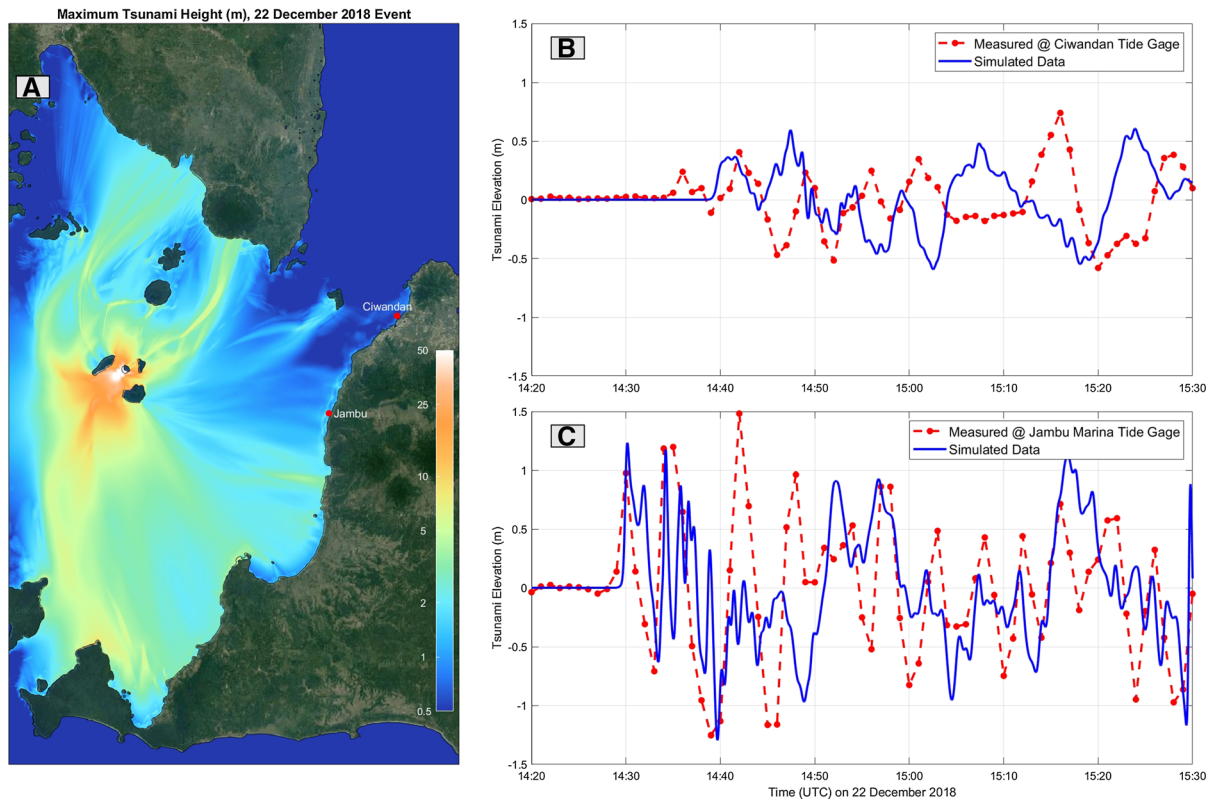
Figure 15
Maximum modelled tsunami heights around the Sunda Strait **a** for the 2018 Anak Krakatau tsunami. Comparison between measured and modelled tsunami heights at Ciwandan (**b**) and Jambu (**c**). In the tide station data (red lines), the red points indicate the measurement sampling rate

explosion type source. However, this source mechanism was discounted by Maeno and Imamura (2011) whose dynamic modelling of pyroclastic flow sources produced a better overall fit to the available data from 1883. While no singular initial maximum tsunami amplitude is given in Maeno and Imamura's (2011) modelling of the pyroclastic flow source, their models are suggestive of initial tsunami heights at the source well in excess of 250 m and their results predict maximum peak to trough tsunami heights of ∼ 120 m and ∼ 40 m at points 8 km north and south of the volcano's center. The results of their modelling thereby support the pyroclastic flow hypothesis put forth by Self and Rampino (1981) and now commonly accepted as the primary tsunami source for that event (Paris 2015).

These results highlight another key difference between the observed effects of the two events in that the 1883 source was directed primarily toward the north while the 2018 event was directed toward the southwest. The northward directivity of the 1883 source is supported by the fact that Rakata Island is the remnant southern end of the former Krakatau Island. This northward directivity likely influenced the observed tsunami effects producing the reported 15–20 m in the Labuhan area, 10 m at Anyer and 37 m runup at Merak whereas as discussed above, the 2018 event pushed tsunami energy to the south producing > 10 m tsunami flow depths at Ujung Kulon. However given the differences in tsunami runup data collection between 1883 and 2018, it is also quite possible that the data reported for 1883 does not provide a complete description of the tsunami effects further reinforcing the assertion that more care must be taken in future studies when discussing the Krakatau tsunamis of 1883.

4. Summary and Conclusions

We conducted a field survey of the areas affected by the tsunami generated following the December 2018 eruption of Anak Krakatoa volcano. Indonesian and international scientists worked together to collect physical data of the tsunami's effects, conduct interviews of affected persons, and provide education on tsunami hazards to the local population. This field survey was the first to collect quantitative tsunami data from the small islands in the immediate tsunami source region.

Our data show that tsunami runup heights exceeded 85 m on the northern coast of Rakata and 83 m on the southern coast of Sertung. In agreement with numerical models, our survey confirmed that there were very strong tsunami effects on the northern shores of Panaitan Island and Ujung Kulon at the far western tip of Java. This data combined with measurements of 9 m runup at Sebesi to the north suggests that the tsunami source was highly directive and supports the hypothesis of a landslide/flank collapse as the causative tsunami generating mechanism.

Numerical modeling of the event incorporated a hot start initial condition derived from empirical formula for landslide generated water waves and a Boussinesq propagation and runup model. We were able to reproduce measured data in both the immediate source area and at tide gauges on the Java coast. The hydrodynamic modelling also accurately predicted areas of wave focusing where higher runup values were measured.

Interviews with witnesses and survivors suggest that the local population was caught largely off guard with respect to the possibility of a tsunami disaster. This despite the extreme tsunami history of the region and the months of heightened volcanic activity preceding this event. This again highlights the need for community-based education and awareness programs as essential to save lives in locales at risk from locally generated tsunamis.

Publisher's Note Springer Nature remains neutral with regard to jurisdictional claims in published maps and institutional affiliations.

REFERENCES

Briggs, M. J., Synolakis, C. E., Harkins, G. S., & Green, D. R. (1995). Laboratory experiments of tsunami runup on a circular island. *Pure and Applied Geophysics, 144*(3/4), 569–659.

Giachetti, T., Paris, R., Kelfoun, K., & Ontowirjo, B. (2012). Tsunami hazard related to a flank collapse of Anak Krakatau Volcano, Sunda Strait, Indonesia. *Geological Society, London, Special Publications, 361*(1), 79.

Grilli, S., Tappin, D., Carey, S., Watt, S., Ward, S., Grilli, A., et al. (2019). Modelling of the tsunami from the December 22, 2018 lateral collapse of Anak Krakatau volcano in the Sunda Straits, Indonesia. *Scientific Reports,.* https://doi.org/10.1038/s41598-019-48327-6.

Heidarzadeh, M., Ishibe, T., Sandanbata, O., Muhari, A., & Wijanarto, A. B. (2020a). Numerical modeling of the subaerial landslide source of the 22 December 2018 Anak Krakatoa volcanic tsunami, Indonesia. *Ocean Engineering.* https://doi.org/10.1016/j.oceaneng.2019.106733.

Heidarzadeh, M., Putra, P. S., & Nugroho, S. H. (2020b). Field survey of tsunami heights and runups following the 22 December 2018 Anak Krakatau volcano tsunami, Indonesia. *Pure and Applied Geophysics* (**submitted**).

Kanoglu, U., & Synolakis, C. E. (1998). Long wave runup on piecewise linear topographies. *Journal of Fluid Mechanics, 374*, 1–28.

Kushendratno. (2019). Pemantauan Visual Letusan Gunung Anak Krakatau Periode Juli-Desember 2018. Badan Geologi Press, Bandung, p. 277–296. Geologi Selat Sunda Book. (https://www.esdm.go.id/id/publikasi/publikasi-hasil-kajian)

Liu, P. L.-F., Cho, Y.-C., Briggs, M., Kânoğlu, U., & Synolakis, C. E. (1995). Runup of solitary waves on a circular island. *Journal of Fluid Mechanics, 302*, 259–285.

Lo, H. Y., & Liu, P. L. F. (2017). On the analytical solutions for water waves generated by a prescribed landslide. *Journal of Fluid Mechanics, 821*, 85–116.

Lynett, P. (2006). Nearshore wave modeling with high-order Boussinesq-type equations. *Journal of the Waterways and Harbors Division ASCE, 132*, 348–357.

Mader, C. L., & Gittings, M. L. (2006). Numerical model for the Krakatoa hydrovolcanic explosion and tsunami. *Science of Tsunami Hazards, 24*(3), 174.

Maeno, F., & Imamura, F. (2011). Tsunami generation by a rapid entrance of pyroclastic flow into the sea during the 1883 Krakatau eruption, Indonesia. *Journal of Geophysical Research: Solid Earth, 116*(September), 1–24. https://doi.org/10.1029/2011JB008253.

Muhari, A., Heidarzadeh, M., Susmoro, H., Nugroho, H., Kriswati, E., Supartoyo, W. A., et al. (2019). The December 2018 Anak Krakatau volcano tsunami as inferred from post-tsunami field surveys and spectral analysis. *Pure and Applied Gepophysics*. https://doi.org/10.1007/s00024-019-02358-2.

NGDC/NCEI/WDS National Geophysical Data Center/World Data Service: NCEI/WDS Global Historical Tsunami Database. NOAA National Centers for Environmental Information. https://doi.org/10.7289/V5PN93H7. Accessed May 2020.

Nomanbhoy, N., & Satake, K. (1995). Generation mechanism of tsunamis from the 1883 Krakatau. *Geophysical Research Letters, 22*(4), 509–512.

Pararas-Carayannis, G. (2003). Near and far-field effects of tsunamis generated by the paroxysmal eruptions, explosions, caldera collapses and massive slopes failures of the Krakatau volcano in Indonesia on August 26–27, 1883. *Science of Tsunami Hazards, 21*(4), 191–222.

Paris, A., Heinrich, P., Paris, R., & Abadie, S. (2020). The December 22, 2018 Anak Krakatau, Indonesia, Landslide and Tsunami: Preliminary modeling results. *Pure and Applied Geophysics, 177*(2), 571–590. https://doi.org/10.1007/s00024-019-02394-y.

Paris, R. (2015). Source mechanisms of volcanic tsunamis. *Philosophical Transactions of the Royal Society A: Mathematical, Physical and Engineering Sciences, 373*(2053), 1–15. https://doi.org/10.1098/rsta.2014.0380.

Putra, P. S., Aswan, A., Maryunani, K. A., Yulianto, E., Nugroho, S. H., & Setiawan, V. (2020). Post-event field survey of the 22 December 2018 Anak Krakatau tsunami. *Pure and Applied Geophysics*. https://doi.org/10.1007/s00024-020-02446-8.

Self, S., & Rampino, M. R. (1981). The 1883 eruption of Krakatau. *Nature, 294*(5843), 699–704. https://doi.org/10.1038/294699a0.

Sutawijaya, I. S. (2006). Pertumbuhan Gunung Api Anak Krakatau setelah letusan Katastrofis 1883. *Jurnal Geologi Indonesia, 1*(3), 143–153.

Titov, V. V., & Synolakis, C. E. (1997). Extreme inundation flows during the Hokkaido-Nansei-Oki tsunami. *Geophysical Research Letter, 24*(11), 1315–1318.

UNESCO (2014) International Tsunami Survey Team (ITST) Post-Tsunami Survey Field Guide, 2nd edn. IOC Manuals and Guides No. 37, Paris: (English)

Verbeek, R. D. M. (1885). The time determination of the biggest explosion of Krakatau on August 27, 1883. Science 3, 1884, h. 43–55, and Arch. Neerl. Haarlem 20, 1885, h. 1–13

Walter, T. R., Haghshenas Haghighi, M., Schneider, F. M., Coppola, D., Motagh, M., Saul, J., et al. (2019). Complex hazard cascade culminating in the Anak Krakatau sector collapse. *Nature Communications, 10*(1), 1–11. https://doi.org/10.1038/s41467-019-12284-5.

Yeh, H., Imamura, F., Synolakis, C. E., Tsuji, Y., Liu, P., & Shi, S. (1993). The flores island tsunamis. *Eos, Transactions of the American Geophysical Union, 74*(33), 369–373.